National Defence
Research and Development Branch

Défense nationale
Bureau de recherche et développement

TECHNICAL MEMORANDUM 96/227
March 1997

REVIEW OF LITERATURE RELATED TO MICROSTRUCTURE DEVELOPMENT DURING LASER SURFACE ENGINEERING OF NICKEL ALUMINUM BRONZE

Calvin V. Hyatt

Defence Research Establisnment Atlantic

Centre de Recherches pour la Défense Atlantique

Canada

DEFENCE RESEARCH ESTABLISHMENT ATLANTIC

9 GROVE STREET
P.O. BOX 1012
DARTMOUTH, N.S.
B2Y 3Z7

TELEPHONE
(902) 426-3100

CENTRE DE RECHERCHES POUR LA DÉFENSE ATLANTIQUE

9 GROVE STREET
C.P. BOX 1012
DARTMOUTH, N.É.
B2Y 3Z7

National Defence
Research and Development Branch

Défense nationale
Bureau de recherche et développement

REVIEW OF LITERATURE RELATED TO MICROSTRUCTURE DEVELOPMENT DURING LASER SURFACE ENGINEERING OF NICKEL ALUMINUM BRONZE

Calvin V. Hyatt

March 1997

Approved by R.S. Hollingshead:
Head/Dockyard Laboratory (Atlantic) Section

TECHNICAL MEMORANDUM 96/227

Defence Research Establishment Atlantic

Centre de Recherches pour la Défense Atlantique

Canada

ABSTRACT

In this report, literature related to the low heat input welding of nickel aluminum bronze is examined. This includes data on phases present, composition effects, phase diagrams, transformation kinetics, and the nature of martensites. Relevant data on microstructure development in castings, wrought materials, conventional welds and low heat input welds is considered. So is related work on the examination of melt spun ribbons and Gleeble studies. Available data show that a martensite with a 9-R structure is common in low heat input nickel aluminum bronze welds over a range of compositions. Other structures are expected at other compositions. Data also show that for at least one alloy composition, formation of Widmanstätten α can be suppressed with a high enough cooling rate ($\Delta t_{800\text{-}500}$ of 1.6 seconds or faster). As well, data show that tempering of martensites in weld heat affected zones probably does not occur at temperatures of less than roughly 400 °C. The review shows that experiments to obtain data on ordering, metastable reactions, precipitation and tempering are needed. Also needed are experiments to understand the effect of composition and heat input on microstructure.

RÉSUMÉ

Le présent rapport passe en revue la documentation sur le soudage du bronze au nickel-aluminium avec faible apport de chaleur: phases en présence, effets des compositions, diagrammes de phase, cinétique de la transformation et nature des martensites. Sont examinées des données pertinentes sur l'évolution des microstructures dans les pièces coulées, les matériaux forgés, les soudures classiques et les soudures avec faible apport de chaleur, ainsi que des études connexes sur les rubans centrifugés à chaud et les Gleeble. Les données disponibles indiquent qu'une martensite à structure 9-R est souvent présente dans une gamme de compositions de soudures en bronze au nickel-aluminium avec faible apport de chaleur. D'autres structures sont prévues dans d'autres compositions. Les données révèlent aussi que, pour au moins une composition d'alliage, il est possible d'empêcher la formation de Widmanstätten a à une vitesse de refroidissement assez élevée ($\Delta t_{800\text{-}500}$ de 1,6 s ou moins), quoique cela soit peu probable dans des alliages pauvres en aluminium. Elles révèlent également que le revenu des martensites dans les zones affectées par la chaleur ne se produit probablement pas à des températures inférieures à quelque 400 °C. Les données sur le classement, les réactions métastables, la précipitation et le revenu s'avèrent incomplètes, et l'effet de la composition et de l'apport de chaleur sur la microstructure est méconnu.

DREA TECHNICAL MEMORANDUM/96/227

Review of Literature Related to Microstructural Development During Laser Surface Engineering of Nickel Aluminum Bronze

by

C.V. Hyatt

EXECUTIVE SUMMARY

Introduction: There is a need to make high value components of ships and submarines last longer and perform better. In many cases, this can be done by treating or changing surfaces to make them more resistant to wear, corrosion and fatigue initiation. For example, laser surface melting and cladding of nickel aluminum bronze, an alloy used in warship and submarine propellers, combat systems equipment and seawater handling systems, gives up to an order of magnitude improvement in such surface properties. There is good reason to believe even larger improvements are possible by designing special purpose consumable alloys optimized for the high cooling rates associated with these processes. Applying these processes in engineering practice requires development of special equipment and procedures, development and application of evaluation methods to assess properties and microstructures, and the development of optimum alloy compositions. One aspect of assessing microstructures and developing optimum alloy compositions is reviewing available literature.

Principal Results: In this report, literature related to the development of microstructures during low heat input welding of nickel aluminum bronze is examined. This includes data on phases present, composition effects, phase diagrams, and transformation kinetics. Relevant data on microstructural development in castings, wrought materials, conventional welds and low heat input welds is considered. So is related work on the examination of melt spun ribbons and Gleeble simulation studies. Available data show that a martensite with a 9-R structure is common in low heat input nickel aluminum bronze welds over a range of compositions. Other structures are expected at other compositions. Data show that for at least one alloy composition, formation of Widmanstätten α can be suppressed with a high enough cooling rate ($\Delta t_{800\text{-}500}$ of 1.6 seconds or faster). Data also show that tempering of martensites in weld heat affected zones probably does not occur at temperatures of less than roughly 400 °C. The review shows that experiments to obtain data on ordering, metastable reactions, precipitation and tempering are needed. Also needed are experiments to understand the effect of composition and heat input on microstructure.

Significance of Results: Low heat welding processes such as laser cladding, are promising methods both for repairing and for surface engineering high value components of Canadian Navy ships. As a repair procedure, low heat input welding offers a means to repair components which cannot now be repaired. As a surface engineering method, low

heat input weld cladding can give order of magnitude improvements in surface properties. These property improvements will give improved component life and performance. The work summarized in this review will allow low heat input welding experiments with conventional nickel aluminum bronze consumables to be better interpreted. It also shows how an optimized low heat input weld deposit might be produced. Possibilities include control of deposit composition and welding heat input to regulate relative amounts of martensite and Widmanstätten α in the microstructure and to optimize precipitate type and distribution.

Future Work: Work on the effect of heat input and composition on the microstructure and properties of the nickel aluminum bronze weld deposits is in progress. At this writing, twenty-seven alloy compositions, each treated with ten different heat inputs are being investigated at the Defence Research Establisment Atlantic. We have already demonstrated that complex parts can be clad. Within three years, we will develop one or more optimized alloy compositions for low heat input welding and characterize them well enough so that they can be used with confidence.

TABLE OF CONTENTS

1.0 INTRODUCTION

In the past few years there have been a number of articles published about the laser surface melting and cladding of nickel aluminum bronzes and related alloys [1-17]. These bronzes have good weldability and because of their multicomponent nature benefit from the homogenization and grain refinement associated with the rapid solidification rates of these processes. Further, upon cooling, these bronzes undergo a phase transformation from high temperature β phase to low temperature α phase. With the rapid post solidification cooling rates associated with these processes, a martensitic or Widmanstätten transformation occurs, along with the precipitation of ordered particles. Significant hardening occurs as a result of these transformations. As well, significant improvements in wear [15], corrosion, cavitation and erosion behavior have been reported [7-10,13,14].

There is good reason to be interested in these results. As castings and wrought products, these alloys see engineering use in a wide range of applications including valves, impellers, propellers, machinery parts, wear or bearing strips, forming tools, bearings, specialized tooling, marine fittings and a number of other applications [18-21]. Deposits of these alloys by conventional welding are used for the repair and reclamation of components made from a range of copper alloys and from other materials, including steels and cast irons. Nickel aluminum bronze is also deposited by spray deposition methods for repair and reclamation, for use as a porous bearing surface and for use as an interlayer prior to the deposition of other materials [21].

The material is used in this wide range of applications because of its excellent combined mechanical, corrosion, wear and fabrication properties. Propellers for large ships are an excellent example. Applicable standards permit higher stresses on these alloys than on any other common propeller casting alloy [19, 22] This is a result of the good toughness, corrosion fatigue resistance, and stress corrosion resistance of nickel aluminum bronzes.

One well known problem with the alloys in certain environments is de-alloying. Though more resistant to this than most other high strength copper alloys, nickel aluminum bronzes are somewhat susceptible. Problems with dealuminification have caused concern and led to a number of changes in practice [23-26]. The problem occurs in valves in seawater systems, especially those which see stagnant conditions, receive little deliberate or incidental cathodic protection, may be coupled to more noble monel or titanium pipes, may have been weld repaired and which have crevices as a result of design or deposits. Such castings are used with the knowledge that corrosion will occur. So long as this corrosion is pitting or impingement attack, nondestructive inspection can be used to identify problems before they become critical. Dealuminification, whether at a crevice or adjacent to a weld heat affected zone is more of a concern because low strength porous copper is redeposited on the affected surface, precluding nondestructive assessment of the depth of attack with acceptable confidence. Rates of attack of 0.25 mm/year at crevices in as cast material and of 1 mm/year in or adjacent to weld heat affected zones have been

reported [26]. Fundamental understanding of both general dealloying and dealloying in aluminum bronzes is still not adequate [27]. Examination of dealloying on a large number of valves suggests a number of variables play a role. In many cases, a mechanism involving an initial transient period, followed by the dissolution of intermetallic lamellae in the eutectoid regions at a more rapid rate than the surrounding α matrix is thought to be active in at least a majority of cases [23]. While heat treatments have been partly successful in eliminating dealuminification, the problems may still occur in very large castings, which have coarse eutectoid structures and in castings which have insufficient Ni [24]. It has been suggested that residual stress plays a role in the preferential attack near weld heat affected zones [24]. Attack of weld metal does not seem to be serious, provided a matching filler metal is selected.

To apply low heat input welding methods to nickel aluminum bronzes, it is necessary to develop the processes, characterize the resulting microstructures and properties and develop alloys which take advantage of the thermal cycles associated with low heat input methods. A difficulty with characterizing microstructures and developing new alloys is a lack of understanding of microstructural development in low heat input welding. This review summarizes all available data relevant to this.

2.0 COMPOSITION RANGE OF NICKEL ALUMINUM BRONZES

A number of different copper alloys are commonly called nickel aluminum bronze. A list of some of the standards which define these alloys is given in Table 1 [18, 24]..In nickel aluminum bronzes the major alloying element are aluminum from 8 to 13 %, nickel from 3 to 5 %, iron from 3 to 5 %, and manganese from 0 to 3 %. Minor elements such as tin and zinc (both <0.2 %) and Si (< 1.0 %) are also present in these alloys. Other elements have been added in experimental bronze alloys to give age hardening (antimony, arsenic, cadmium, chromium, indium, phosphorous, tin, titanium, vanadium and zirconium) and resistance to stress corrosion (cadmium, arsenic and zirconium) [21]. Some workers have proposed formulas to relate properties to an equivalent Al+Mn/X, with the X varying from 4 to 8 [30]. A similar formulation has not been given for hardenability

TABLE 1. NICKEL ALUMINUM BRONZE STANDARDS [Compositions from refs 18, 28, 29]

STANDARD									ALLOWED COMPOSITION RANGE					COMMENT	
BS	DGS	AUWE	DTD	DIN	ASTM	UNS	ISO	MIL	AWS	Al	Fe	Ni	Mn		
CA104			197A	17665: CuAl10Ni	B150 63200	C63200	428 CuA110Fe5Ni5			8.5-11.0	4.0-6.0	4.0-6.0	3.5 max		Wrought Alloys
CA105					B171 63000	C63000				8.5-10.5	1.3-3.5	4.0-7.0	0.5-2.0		"
				17665: CuA11Ni						10.5-12.5	4.8-7.3	4.0-7.0	(?)		"
	1043	930.14								8.5-10.0	4.0-5.5	4.0-5.5	3.5 max(?)		"
AB2	361A	930.3		1714: CuAll0Ni			1338 CuAll0Fe5Ni5			8.5-10.5	3.5-5.5	4.5-5.5	(?)		Casting Alloys
	8520F	930.15								8.8-9.5	4.0-5.0	4.5-5.5	(?)		"
			174							7.5-10.5	1.5-3.5	4.0 max	(?)		"
			412							8.0-12	3.0-6.0	3.0-6.0			"
	348									8.8-9.5	4.0-5.0	4.5-5.5	0.75-3.0		"
	(NES747)									8.9-9.6	4.0-5.0	4.5-5.5	1.0-1.4		"
					B148 95500	C95500				10-11.5	3.0-5.0	3.0-5.5	3.5max		"
					B148 95800	C95800		Mil-B24480		8.5-9.5	3.5-4.5	4.0-5.0	0.8-1.5	Ni>Fe	"
								Mil-B-3921		8.5-11.0	3.0-5.0	3.0-5.5	3.5max	Obsolete	"
								Mil-B-2120A		8.5-9.5	3.00-5.00	4.00-5.50	3.5max	Obsolete	"
									ERCuNiAl	8.5-9.5	3.0-5.0	4.0-5.5	0.6-3.5		Welding Wire
									ECuNiAl	6.0-8.5	3.0-6.0	4.0-6.0	0.5-3.5		"
C20										8.0-9.5	1.5-3.5	3.5-5.0	0.5-2.0		"

3.0 COMPOSITION, MORPHOLOGY AND CRYSTALLOGRAPHY OF PHASES IN NICKEL ALUMINUM BRONZE

Table 2. Phases in Nickel Aluminum Bronze castings and wrought products.

Designation	Description	Crystallographic Structure		Ref.
α	Copper rich solid solution	fcc	A1	31
β	High temperature solid solution	bcc	A2	31
κ_I	Cored iron rich particles	Several structures including iron rich bcc, $Fe_3Al(D0_3)$ and FeAl(B2)		32,33
κ_{II}	Iron rich particles (Fe_3Al)	BiF_3	$D0_3$	31
κ_{III}	Nickel rich (NiAl)	CSC1	B2	31
κ_{IV}	Fine iron rich particles (Fe_3Al)	BiF_3	$D0_3$	31
γ_2	Intermetallic compound of wide solubility range. May not form in nickel aluminum bronze. Cu_2Al	γ brass	$D8_3$	31
Particles in retained β	NiAl type	CsC1	B2	32

The phases found in nickel aluminum bronze castings and wrought products are listed in Table 2, along with their crystal structures. Table 3 gives data on compositions of these phases determined on a number of alloys. All used alloys of approximate composition Cu-9.1±0.4Al, 4.4-4.9Ni, 4.4-5.3 Fe, 0.9-1.2 Mn and less than 1 Si. Figure 1 shows a typical cast microstructure and Fig. 2 shows a sketched microstructure which shows the phase relationships of the alloy. The microstructures shown in Fig. 3 are transformation products of the high temperature β phase, which has a bcc crystal structure without chemical order. The low temperature solid solution (α) may occur in a number of morphologies including the single phase and coupled eutectoid regions shown in Fig. 1 and grain boundary and Widmanstätten α forms analogous to those in steels[34]. There is data from a number of workers which shows that on rapid cooling, in binary nickel aluminum bronzes, α platelets form from β by a bainitic (shear plus diffusion) mechanism. The transformation product thus produced is characterized by a Widmanstätten morphology, supersaturation of aluminum, relief due to shear processes and stacking faults [31]. In general, this transformation product forms along with martensite, the β which remains to transform to martensite being enriched somewhat in aluminum. Bainitic plates become finer with increasing aluminum in binary alloys [31]. Identification of

bainitic transformations in more complex alloys, such as the nickel aluminum bronzes, is more difficult because of the complications of competing precipitation reactions [31].

Table 3. Compositions of particles in nickel aluminum bronze castings and wrought products.

Phase	Cu	Al	Fe	Ni	Mn	Si	Ref.
γ_2	85.4 85.8	8±2 7.2±0.4	2.7±2 2.8±0.3	2.5±1.4 3.0±0.2	1.2±0.3 1.1±0.1	<0.1	32 33
κ_I	15±5 9.5	13±5 10±1.3	55±7 72±14	15±3 3.5±.4	2±0.4 2.9±0.5	1.6±0.4	32 33
κ_{II}	19 12.1±3	19 12.3±1.3	32±3 61.3±4.9	27±5 8.0±1.8	2 2±4	— 4.1±.8	32 33
κ_{III}	26±4 17±5	20±4 26.7±1	30±3 12.8±1.6	32±2 41.3±6	1.8±0.4 2.0±0.4	— <0.1	32 33
κ_{IV}	14±5 2.6±7	15±5 10.5±1.7	62±6 73±2	10±5 7.3±1.5	1.3±0.4 2.4±0.2	— 4.0±1.5	32 33
Retained β	85	8.7	1.6	3.5	1.0		32
γ_2	72-76 ~80	14-18 ~17.5	~1	3.5-6			in Cu-Al-Ni 31 in Cu-Al-Fe 31
Particles in retained β	20±4	28±1	14.0±6.0	35±9	2.2±0.3	0.4±03	37

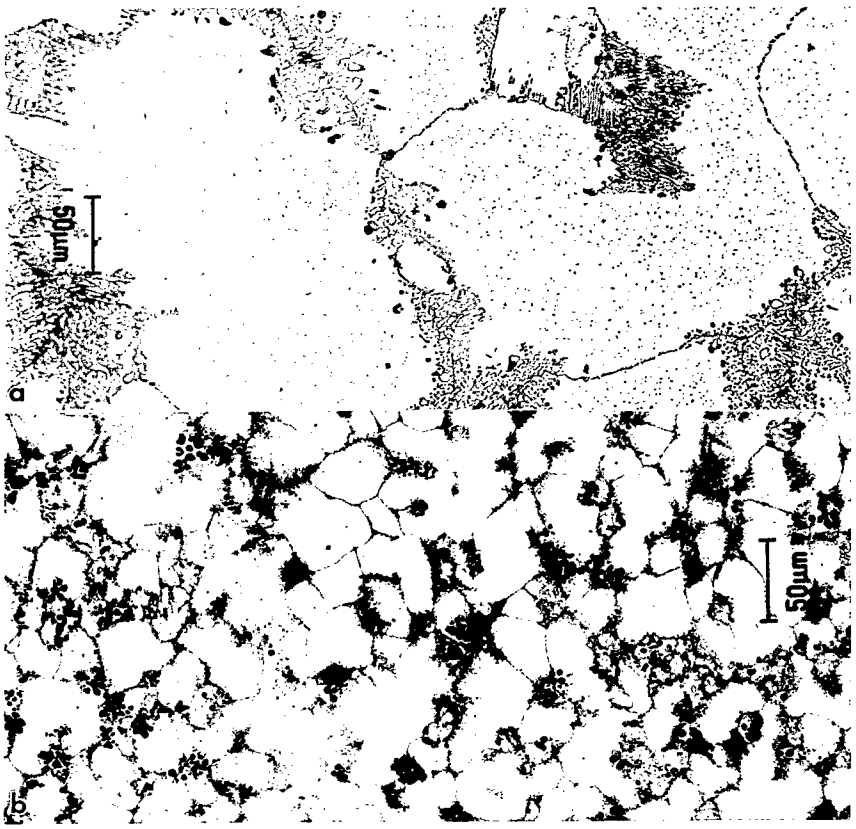

Fig. 1. Microstructure of two cast nickel aluminum bronzes. a. Cu-8.7Al, 4.4 Fe, 4.8 Ni, 1.4 Mn. b. Cu-8.2 Al, 8.4 Fe, 4.15 Ni, .98 Mn.)

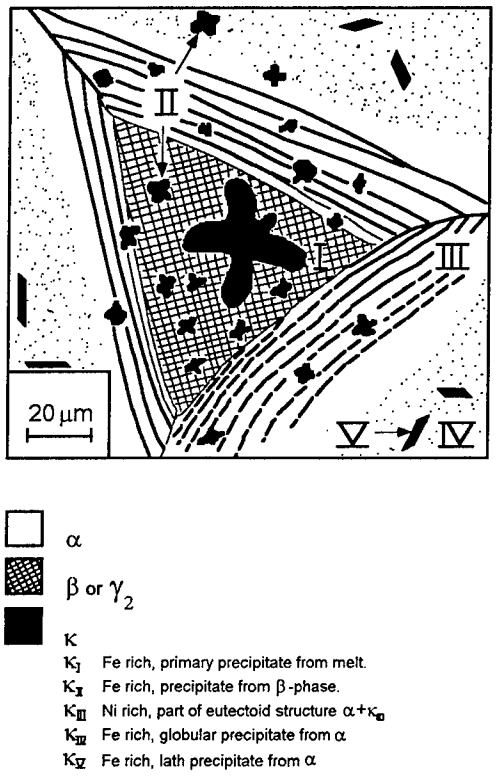

Fig. 2. Schematic of phases in nickel aluminum bronze, from Ref. 31.

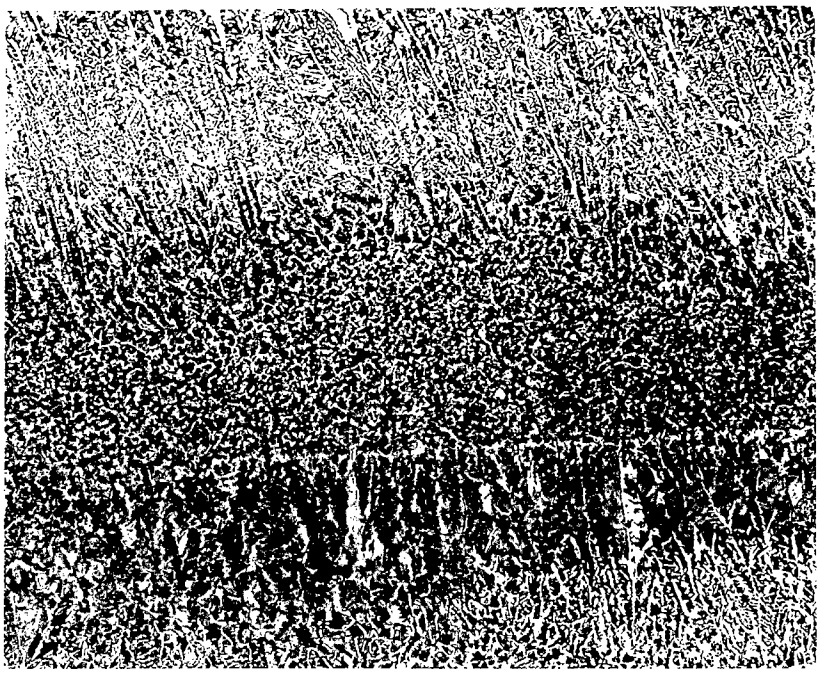

Fig. 3. Martensite (dark) and Widmanstätten, intercritical and grain boundary α (white) in an alloy laser clad with a heat input of 800 J/ cm.

Characterization and categorization of the kappa phases in nickel aluminum bronzes was for some time a controversial topic. The four kappa particles listed in Tables 2 and 3 are identified with a scheme based on morphology proposed by Brezina[1] [31]. A paper by Hasan, Jahanafrooz, Lorimar and Ridley [33], reconciles data on thermodynamics, diffraction and microanalysis studies. They show that the κ_{II} and κ_{IV} particles are the same phase, albeit with slightly different composition, probably because they form at different temperatures, from a matrix of different composition. They show that the κ_{II} and κ_{III} phases are probably different phases. This refutes earlier work by Thompson and Edwards [36], which suggested they were different composition extremes of the same phase. The κ_I particles, which form only in iron rich materials, are cored and in regions of different composition have different structures, as shown in Table 3[2]. Tempering of cast nickel-aluminum bronze at about 675 °C produces a large number of precipitates with a NiAl structure, either in the α matrix or on pre-existing particles of Fe_3Al type [37]. These are probably the particles which Culpan and Rose [32] designated κ_V, though they are the same phase as kappa κ_{III}, and the κ_V designation is rarely used. Orientation relationships for these particles are given in Ref. 37. Unidentified ordered particles have been reported in weld metal of laser welds [5,6].

---

[1] Often this scheme is ascribed to Weil-Couly and Armaund [35]. However, their paper attributes this to Brezina's unpublished thesis.

[2] It is significant to note that in ternary Cu-Al -Fe alloys richer in iron than 5 %, iron rich primary dendrites of unidentified structure do form. It is likely that at least part of the κ_I particles also form this way [31].

The γ_2 (also called δ) phase is well known in binary copper aluminum alloys. In these alloys, when present, especially as a eutectoid, it gives poor corrosion resistance and degraded mechanical properties. It has long been reported that an optically unresolvable γ_2 eutectoid phase is present in the retained β regions of castings, and welds, particularly those with high aluminum, and subjected to slow cooling [38]. However to date, a truly convincing study to show this has not been reported. In all reported work, identification of the γ_2 phase has been by optical methods. It is likely that in at least some cases the regions identified as γ_2 were in fact γ_2. In the only comprehensive study in which transmission electron microscopy and diffraction were used, Hasan, Jahanafrooz, Lorimar and Ridley have shown that the retained β phase in two different castings is a martensite containing precipitates of the same structure as the κ_{III} phase [33].

There is limited data on the nature of martensites in nickel aluminum bronzes. A region of retained β studied by Hasan, Jahanafrooz, Lorimar and Ridley [33] was shown by them to be a 3R (ABABAB) or 2H (ABCABCABC) type[3] martensite. Hansan, Lorimar and Ridley [39] examined a martensite from a weld which gave selected area diffraction patterns consistent with a 9R structure. Liu and coworkers [16,17] examined martensite in a laser deposited nickel aluminum bronze and found it to be a close packed structure, with what was predominately a 9 layer stacking mode(9R) (ABCBCACAB), with occasional local presence of an 11 layer stacking mode (ABCBCACABAB). Long range chemical ordering in the martensites was not detected by Liu and coworkers. Martensites without chemical long range order are found in binary aluminum bronzes with between 8 and 11% Al. Between 11 and 13 % Al, in binary alloys, the martensite is the long range ordered 18R variant [40]. It is relevant to note in this discussion that: the retained martensite discussed by Hansen Jahanafrooz, Lorimar and Ridley was lean in nickel, iron and aluminum relative to the alloys average composition [33]; the martensite characterized by Liu and co-workers formed in an alloy (9.8 Al, 2.2 Fe, 5.3 Ni) lean in iron [16,17]; and that CCT curves presented by Brezina [31], as well as TTT curves for a number of nickel aluminum bronzes suggest the ordering of the β phase occurs before the martensite start temperature. This is significant for two reasons. First, it suggests that martensites in some alloys may have an ordered structure. Second, 18R martensites which form from an ordered bcc parent, are usually thermoelastic, that is they undergo a reverse martensite to parent transformation [39]. The high density of precipitates reported in some nickel aluminum bronze martensites could well impede such a transformation. However, the possibility of the occurrence of such a transformation has implications for alloy design and for the tempering behavior of nickel aluminum bronze martensites. Brezina [31] suggests the retransformation behavior occurs in at least some nickel and iron rich aluminum bronzes.

[3] This terminology describes the stacking sequence of the {110} planes of the martensite parent in the martensite. These stacking sequences are shown in brackets in the main text. Martensites of type 3R and 2H contain internal twinning and those of 9R and 18R contain internal faulting [34, 39 and references therein].

4.0 PHASE DIAGRAMS

Before considering data on nickel aluminum bronzes, it is instructive to consider data on simpler alloys. A binary copper aluminum phase diagram is shown in Fig. 4. Binary aluminum bronzes are classified into non-heat treatable α aluminum bronzes containing between 5 and 8 % Al and complex, heat treatable aluminum bronzes containing more than 8 % Al. A martensitic transformation is possible only in alloys richer in aluminum than 8 %. The type of martensite which forms is dependent on aluminum content. Between 8 and 11 % Al an ordering reaction prior to the formation of martensite does not occur and the martensite which forms is denoted β'. Between 11 and 13 wt % Al, ordering to β_1 occurs before the martensite transformation and an ordered martensite (β_1') forms. In alloys containing between 13 and 15 wt % Al, the β_1 structure decomposes to γ', an internally twinned orthorhombic martensite [40]. On slow cooling, the development of microstructures in complex aluminum bronzes occurs by a eutectoid reaction which produces an α plus γ_2 coupled eutectoid structure, which gives poor mechanical and corrosion performance.

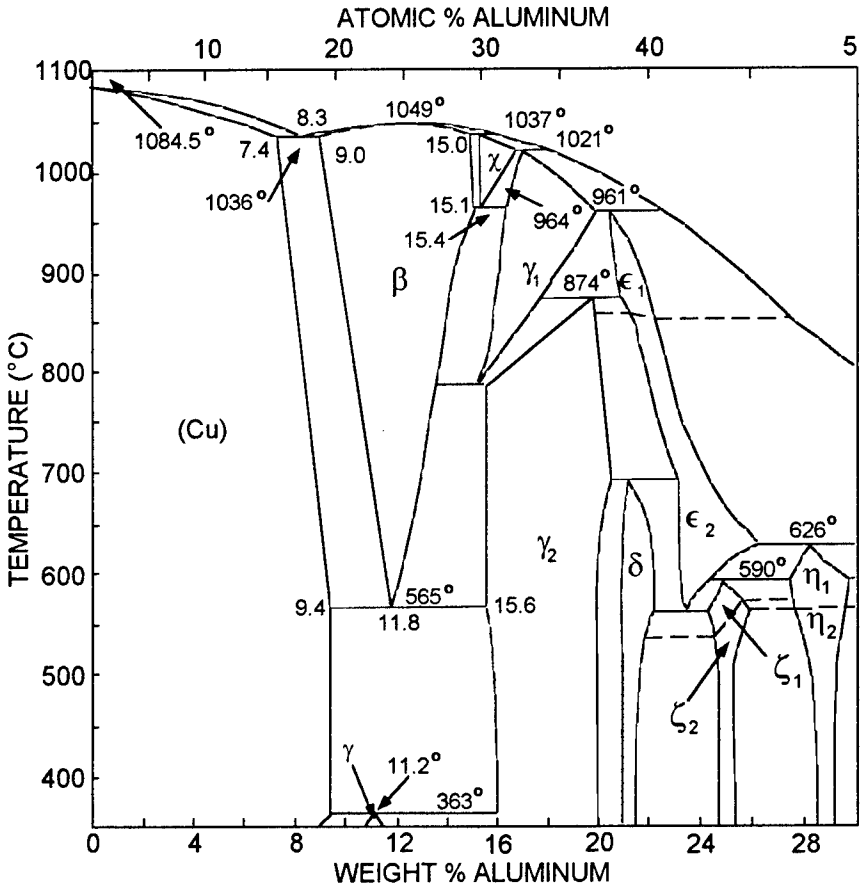

Figure 4. Copper Aluminum Phase Diagram.

Some relevant ternary sections are shown in Fig. 5. They provide little additional insight, except to show that in copper aluminum iron alloys the liquidus temperature is quite high. This suggests that in iron rich nickel aluminum bronze alloys, at least part of the κ_I particles form from the melt. Additional ternary data, including ternary liquidus surfaces are given in Ref. 41. They provide additional support for the conclusions of Hasan and co-workers [33], that the κ_{III} particles are a different phase than the κ_{II} and κ_{IV} phases.

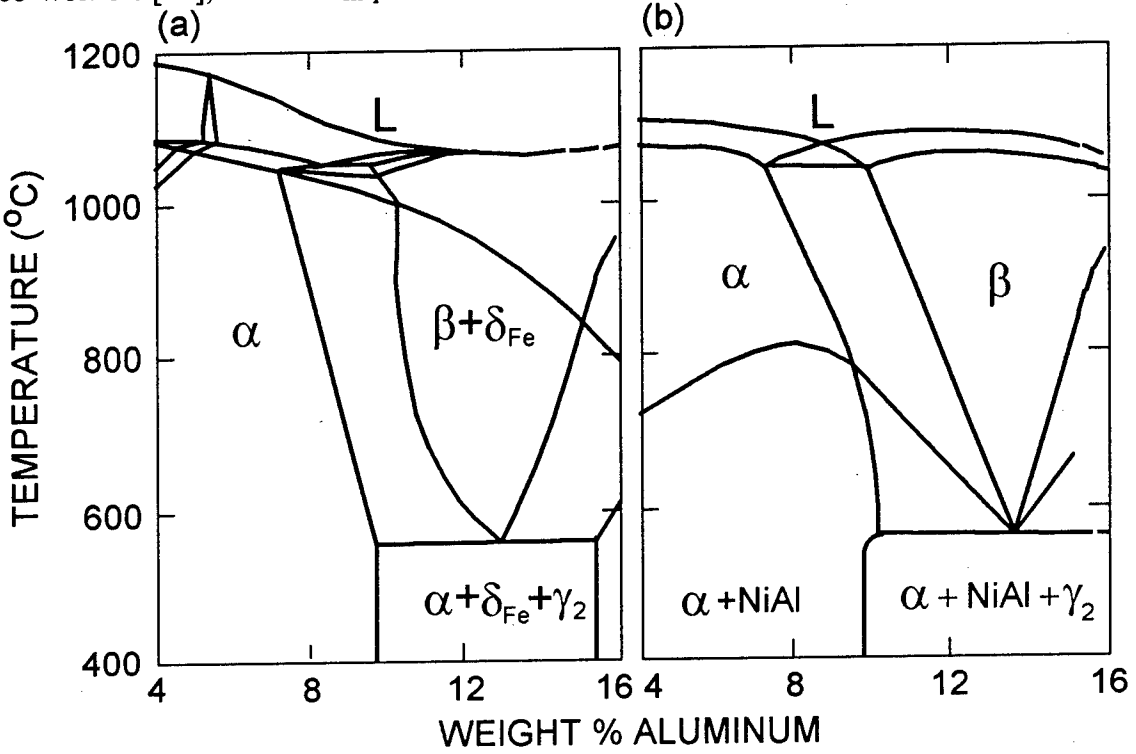

Figure 5. Ternary phase diagram sections from Ref. 31. a. Cu-Al, 5% Fe. b. Cu-Al, 6 % Ni.

Phase diagrams, actually pseudo-binary sections of phase diagrams, for nickel aluminum bronzes have been examined by a number of workers [31,38,42,43,44]. Most have used metallographic techniques only and, though generally aware that there are differences in kappa particle morphology and composition, have made no attempt to display this information on the diagram. The excellent paper by Cook, Fentiman and Davis[38]) provides insight into both constitution and tempering behavior of alloys following solid state quenching. Their diagrams are shown in Fig. 6. They examined alloys which contained from 8-12% Al, and 4-6% each of nickel and iron. Their quenching experiments were done from a maximum temperature of 1000 °C. Because this is about 40 degrees less than the solidus temperature, no insight into solidification behavior is provided. They note that for these alloys, except for the presence of the kappa phases and a shift in the position of the eutectoid, vertical sections of the nickel aluminum bronze phase diagram are generally similar to the aluminum bronze phase diagram [Fig. 4], taking into account consumption of aluminum during the formation of the kappa particles. Kanamori, Ueda and Matsuo show a vertical section of a Cu-Ni-Al-Fe phase diagram for an alloy containing 5 Ni and 5.5 Fe for temperatures less than 1020 °C [43]. It shows

reasonable agreement with the work of Cook and coworkers [38], except in the region between 8 and 12 % Al and 900 to 1000 °C. Brezina [31] shows a vertical section at 5 Ni 5 Fe, Fig. 7, which reasonably agrees with Cook and coworkers [38] and Kanamora and coworkers data [43], except in the region from 8 to 12 % Al and 900 to 1000 °C, where it differs from both. Because Brezina [31] has investigated seven distinct alloy compositions in the range of disagreement, compared with 5 for Kanamora and coworkers [43], and four for Cook and coworkers [38], and because Brezina [31,42] has used both metallographic and thermal analysis methods, while other workers have used only metallography, his diagram seems most suited for future discussions, provided nickel and iron compositions are close to those he describes. As shown in Fig. 7, Brezina's data extends to the liquid state.

The phase diagrams for the binary copper-aluminum system and for the more complex ternary, quaternary or higher systems show neither order start and finish temperatures nor martensite start and finish temperatures. However, for specific compositions there is data on both on continuous cooling transformation (CCT) curves and (time temperature transformation) TTT curves [31,45]. This data is discussed in the next section.

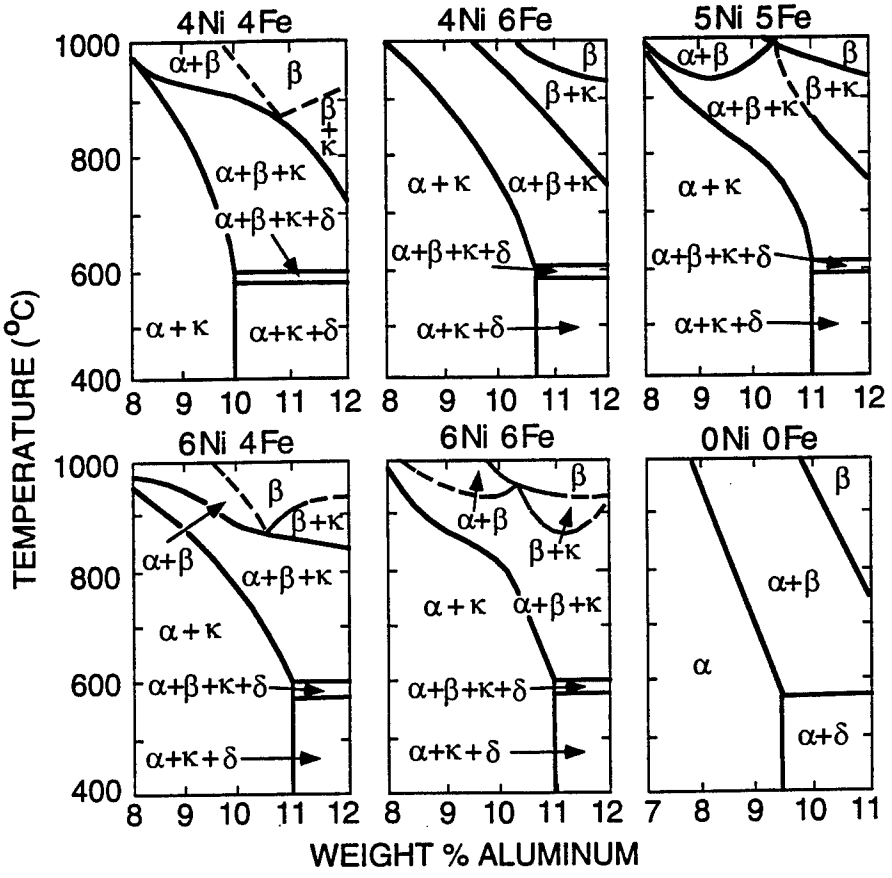

Fig. 6. Vertical section of Cu-Al-Fe-Ni equilibrium diagrams from Cook and coworkers [38].

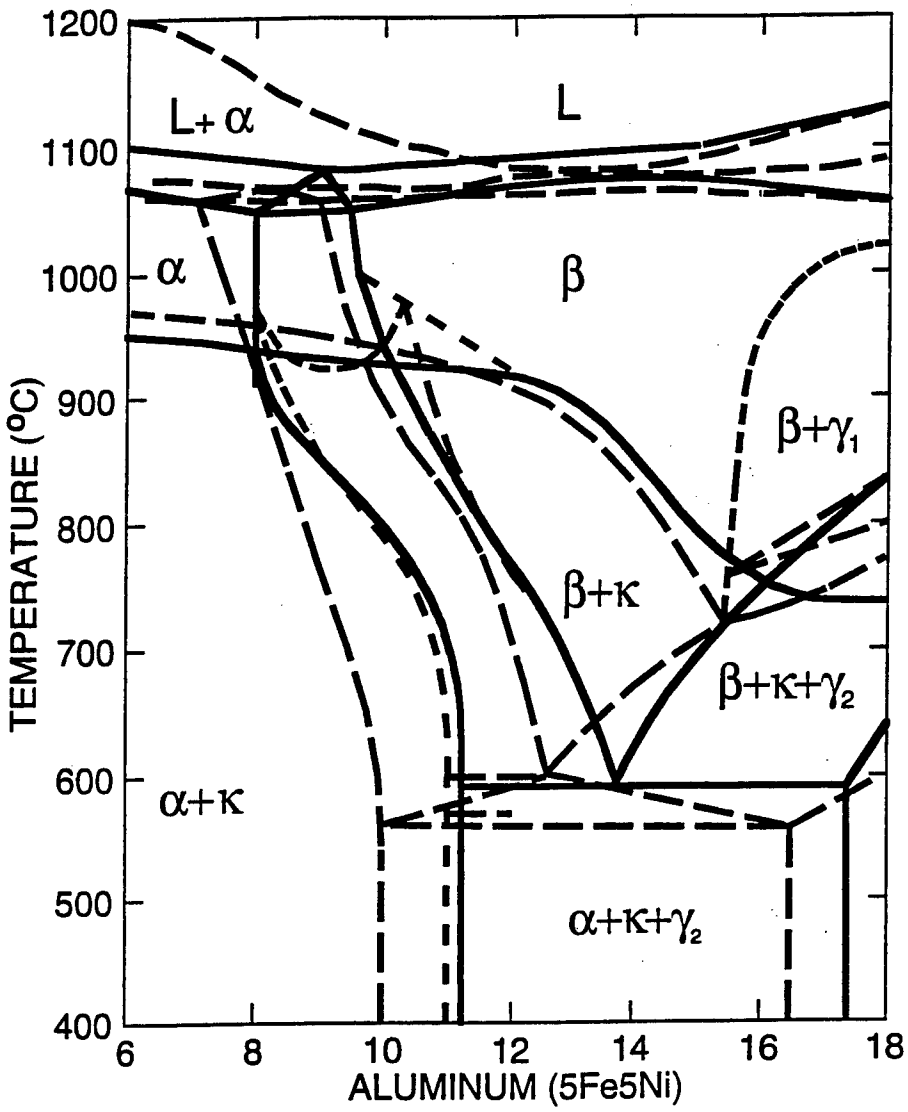

Fig. 7. Vertical section of Cu-Al, 5 Ni 5 Fe equilibrium diagram from Brezina [31]. The unbroken lines are Brezina's data, the short dashed line are from Cook and coworkers data for a similar composition [38], and the long dashed lines are from Rhininsland and Wachtels data for a 3.2 Ni, 4.8 Fe alloy [44].

5.0. KINETICS OF PHASE TRANSFORMATIONS

Data on the kinetics of phase transformations in nickel aluminum bronzes is somewhat limited. Phase transformations on both cooling and tempering are relevant. Brezina summarizes continuous cooling data for several nickel aluminum bronze compositions [31]. These are summarized in Fig. 8. The curves are incomplete and in most cases, the noses are missing. Time temperature transformation curves for a number of aluminum bronzes are given in the Atlas of Time Temperature Transformation curves [45]. The only data which can be compared with Brezina's work is a TTT curve for a Cu-Al-Fe alloy; this

agrees fairly well considering Brezina's [31] curves are for continuous cooling and the other data is from isothermal experiments. From Brezina's work, the martensite start temperature is about 200 °C. Brezina's [31] curves show an ordering reaction β to β_1 occurs at about 400 °C, prior to the martensite transformation, in nickel aluminum bronzes containing 9 to 12 wt % Al. It is relevant to note that, the CTT curves of Brezina are for a solid state transformation, and that the composition of the fraction of the microstructure which transforms to martensite may be somewhat different than the bulk composition, depending on cooling rate. For example, Moon and Garwood [46] have shown that segregation can lead to different ordering peaks in thermal analysis of binary Cu-Al bronzes of a variety of compositions. Brezina also summarizes a number of significant experimental difficulties with the determination of such curves. Still, Brezina's curves are the only presently available source of time-temperature cooling data. More generally, data on TTT curves for binary aluminum bronzes suggests that if the ordering reaction is suppressed the martensite start temperature will be depressed [45]. A differential scanning calorimetry study, by Eucken and coworkers [47], on melt spun ribbons of Cu-12.8 Al, 3.3 Ni suggests this occurs. It shows that as the ribbon cooling rate goes up the martensite start and finish temperatures go down, as do the reverse transformation temperatures, martensite to high temperature β phase start and finish. The temperature shifts over wide ranges of cooling rates, are between 10 and 40 °C. Moon and Garwood have shown that for several Aluminum bronzes, suppression of the β to β_1 ordering reaction does not occur at quenching rates as high as 2000 °C [46]. This is substantially lower than cooling rates likely in the melt spun ribbons, but may approach or even exceed that seen in laser cladding.

Data on tempering of martensites and other β decomposition products is limited. Examination of tempering transformation curves for binary and ternary aluminum bronze alloys, shows significant breakdown of the martensitic structure to α does not occur until above 375 °C [31,45]. It is relevant to note from Brezina's continuous cooling transformation diagrams that this is the temperature regime where Widmanstätten α forms. It is also relevant to note that for binary alloys, the reverse transformation occurs at a temperature above the temperature at which formation of α occurs on tempering. Data on tempering of aluminum bronze shows that retransformation behavior occurs in competition with growth of other phases at some temperatures [48]. It also suggests that in at least some alloys under some conditions, needle-like precipitates of α form within martensite grains after martensite start, and that these needles subsequently coarsen [49].

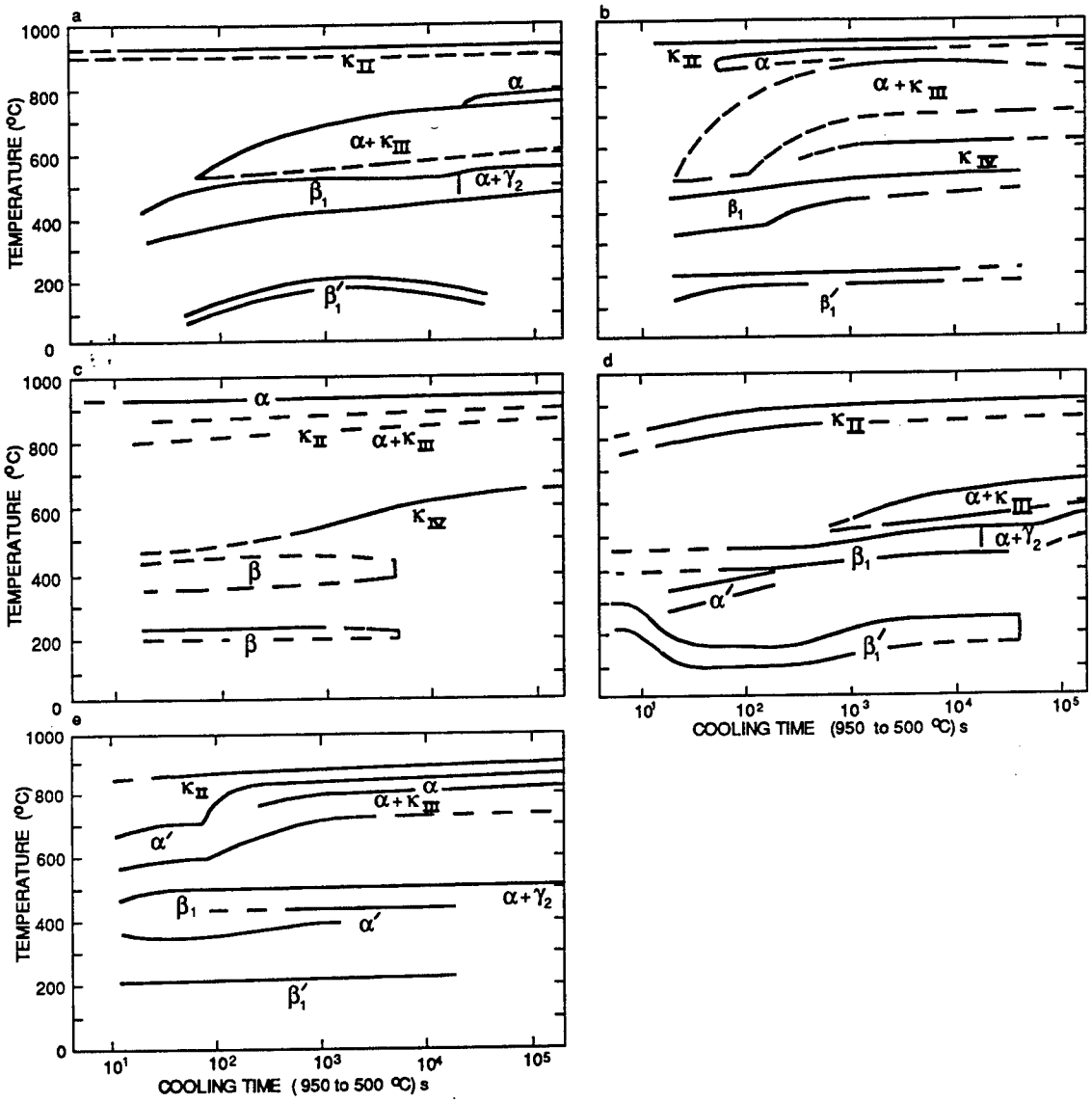

Figure 8. Continuous cooling transformation curves for several nickel aluminum bronzes from Brezina [31]. a. Cu-11.5 Al, 5.3 Fe, 5.1 Ni, 0.9 Mn. b. Cu-9.9Al, 5.3 Fe, 5.1 Ni, 0.9 Mn. c. Cu-8.8 Al, 5.4 Fe, 5 Ni, 0.9 Mn. d. Cu-12.5Al, 4.9 Fe, 5.1 Ni. e. Cu-10.5 Al, 4.6 Fe, 5.0 Ni.

6.0 MICROSTRUCTURAL DEVELOPMENT IN CASTINGS, WROUGHT MATERIALS AND HIGH HEAT INPUT WELDS

6.1 Castings

The development of cast microstructures in these alloys has been studied extensively [for example Refs. 24,33}. Briefly, solidification occurs by nucleation and growth, from the melt, of the high temperature β phase. In iron rich alloys, part of the κ_I particle forms from the melt prior to β phase precipitation. During post solidification cooling, the high temperature β phase transforms to a face centered cubic solid solution designated α, several intermetallic phases, and regions which have traditionally been called retained β (either some type of martensite or, possibly, a metastable α plus γ_2 eutectoid product, as discussed in Section 4). Regardless of the precise form of the retained β transformation products, the regions where these β transformation products form are generally the last area of as-cast β to transform. Partitioning of alloying elements during earlier transformations leaves these regions with a different composition than the surrounding material [33]. Heat treatment of nickel aluminum bronze castings is sometimes done to eliminate these regions and to break up the continuous eutectoid regions. From the perspective of low heat input welding, what is significant is that regions of different composition, may give different local heat affected zone and fusion zone compositions, and thus different local behavior. These effects are expected to be different in castings of different composition, for example the presence or absence of κ_I is determined by composition, and by different thermal history.

6.2 Wrought Products

Cook, Fentiman and Davis [38], Macken and Smith [21], and others [5,6,50,51] have discussed development of microstructures in hot rolled and hot rolled and annealed plates of various composition. In general microstructures consist of fine kappa and α with distorted kappa rosettes in the as hot rolled condition. Banding, analogous to that in rolled carbon manganese steel commonly occurred. Significant variations in hardenability were reported to occur across this banding.

6.3 Conventional Welds

Nickel aluminum bronze is a weldable alloy. There is a significant amount of practical information on welding of this alloy [18,21,28,29,52-56]. In conventional arc welding microstructural development in nickel aluminum bronze is complex and depends strongly on composition, heat input, and welding sequence (as it affects transformations caused by reheating). As deposited, weld metal is usually reported to be Widmanstätten α in a matrix of dark etching retained β phase [for example 52,53]. The nature of the retained β phase is often not described, or at least not completely characterized. Instead, usually implicitly, the approach has been that described by Breznia [31] in which the nature of the

transformation products from the high temperature phase are identified as β^*, without describing them precisely.

Regardless of the microstructure of the as deposited material, reheating by subsequent passes tempers the reheated (interpass heat affected) zones. The products of this tempering may include eutectoidal mixtures of α and κ_{III}, and γ_2, as well as isolated α and intermetallic compounds of various compositions. Post weld heat treatment modifies structure as well.

7.0. MICROSTRUCTURAL DEVELOPMENT IN LOW HEAT INPUT WELDING

There is limited information, produced by four groups [5,6,16,17,39,57], related to the development of microstructures in low heat input welding of nickel aluminum bronze. Hansan and coworkers [39] investigated the heat affected zone produced by electron beam welding of a Cu-10Al, 5%Ni, 5%Fe cast alloy. The heat input was about 1300 J/cm. The size of the heat affected zone, from fusion line to unaffected base material was about 300 μm. They reported that, within the heat affected zone:

> (i) the dark etching eutectoidal phase was replaced with dark etching zones which were featureless when examined with optical microscopy, the κ_{IV} particles changed from being round to elongated, and the dendritic κ_{II} particles became rounded;
>
> (ii) the dark etching regions were a martensite which gave selected area diffraction patterns consistent with a 9-R structure containing partially dissolved κ_{II} particles, the elongated κ_{IV} particles were either a core of κ_{IV} with the original Fe_3Al structure surrounded by a martensite (which gave selected area diffraction patterns consistent with a twinned 9R structure), or entirely martensite, depending on prior size and distance from the fusion line; and
>
> (iii) the volume fraction of dark etching martensite phase dropped with distance from the fusion zone, as did the spherodization of the κ_{II} particles.

It is significant that martensites in the low heat input welds are substantially different from those observed in the cast structures and associated with poor dealloying resistance. Brezina summarizes data which suggests that low aluminum martensites are more resistant to dealloying than high aluminum martensites and that as β decomposition products become finer, the resistance to dealloying goes up [31].

Bell [5] and Pertrolonis [6] and coworkers [50,51], examined microstructural development in both wrought and cast nickel aluminum bronzes at heat inputs in autogenous laser welding from 2 to 13.8 kJ/cm. The results of their transmission electron microscope studies on microstructural characterization were in substantial agreement with

those of Hasan and coworkers [39]. They noted that there was a transition from a columnar to an equiaxed structure within the weld deposit as the weld centerline was approached. They also noted that base metal microstructure, whether wrought or cast, had a strong effect on the structure of the heat affected zone. In the cast material, a mixture of martensite and Widmanstätten α was observed within the heat affected zone. In the wrought material, the prior banded structure produced a heat affected zone with alternating bands of α and martensite.

Liu and coworkers [16,17] characterized a deposit produced by laser cladding aluminum bronze powder containing 9.79 Al 2.19 Fe, 5.27 Ni onto an aluminum-silicon alloy casting alloy. A heat input of 2.8 kJ/cm was used and analysis revealed dilution to be minimal. They examined the morphologies of the weld deposits including martensites and precipitates and examined the tempering behavior of the alloy with microscopy and differential thermal analysis. They reported two martensites were present in the weld deposit, and called them, based on their morphology, sheet and lath martensites. The sheet martensite was determined to be a close packed structure, with what was predominately a 9 layer stacking mode (ABCBCACAB), with occasional local presence of an 11 layer stacking mode (ABCBCACABAB). The lath martensite was identified to have an FCC structure and was shown to contain a high density of stacking faults. Chemical ordering in the martensites was not detected. Precipitates were reported in the sheet martensite phase. They were spherical, but, upon heat treatment at 673 °K for 4 hours became rod like. Differential thermal analysis showed significant precipitate growth occurred between 523°K and 723°K. Microscopy revealed there was little change in stacking fault or dislocations on tempering at 673°K.

It appears that what Liu and coworkers [16,17] call lath martensite is in fact the α phases referred to by other authors as Widmanstätten α. Liu and coworkers do not present evidence to show that the so called lath martensite phase actually forms by a diffusionless process. A naming convention and more understanding are needed here.

Hyatt and coworkers [1-3] studied laser surface melting and cladding of nickel aluminum bronzes using heat inputs from 10 to 6000 J/cm and a range of alloys. The microstructures produced in this work depended on processing method and conditions, and on material composition. At the lowest heat inputs, below 425 J/cm, for alloys containing more than about 9 % Al, deposits were largely martensite. As heat input increased, first grain boundary, and then Widmanstätten α, at about 600 J/cm, formed in the deposit as well. Also with increasing heat input; the amount of grain boundary and Widmanstätten α in the reheated or interpasss heat affected zone increased.

In work to be published soon, Bennet and Hyatt [57] performed a series of experiments to characterize different regions of a laser clad surface produced by cladding an 8.6 Al, 4.8 Ni, 4.0 Fe, 1.1 Mn alloy with a heat input of 1200 J/cm and a welding wire of composition 9.0 Al, 4.6 Ni, 3.9 Fe and 1.2 Mn. Specimens were removed from regions of the weld identified by optical microscopy. A significant observation was that the martensite phase in the deposit contained a high density of ordered precipitates. A question still to be

answered is whether the ordering reaction reported on Brezina's CCT curves is in fact formation of these precipitates.

It should be noted that direct comparison of the heat inputs in the work of Hansen and coworkers [39]; Bell, Petrolinis and coworkers [5,6,50,51], Liu and coworkers [16,17], and Hyatt and coworkers [1-3,56] is not possible with current knowledge because process efficiencies are unknown but different and compositions differ. The geometry of the weld examined by Hansen and coworkers [37] was not reported, so efficiency is between 0.6 and 0.9. The welds of Bell, Petrolinis and coworkers [5,6,50,51] were made autogenously with laser welding in the keyhole mode (which is unsuited to surface treatment). This is a much higher efficiency process than that used by Hyatt and coworkers [1-3,56] in surface melting and cladding with a wire feed in conduction mode. Liu and coworkers [16,17] used conditions that were different from other workers, because they used a powder feed cladding mechanism (which is expected to improve efficiency) and the substrate used was an aluminum alloy with 3 to 5 times higher thermal diffusivity, giving more rapid cooling.

8.0 RELATED WORK ON MICROSTRUCTURAL DEVELOPMENT

There is a limited amount of relevant related work on microstuctural development in nickel aluminum bronzes. Brezina's extensive review article gives information on the solid state heat treatment of nickel aluminum bronze [31]. For engineering purposes, solid state heat treatment of nickel aluminum bronzes usually involves quenching from about 900 °C followed by tempering at 600 °C for up to 4 hours. He provides much data of more fundamental interest as well. Data on continuous cooling transformation behavior and on tempering behavior were discussed in Section 5. Relevant other results summarized by Brezina include:

1. Observations that a massive transformation can be induced in binary alloys of composition Cu-8.5 to 9.5Al, by brine quenching of specimens less than 2.5 mm thick;

2. In ternary alloys, Iron stabilizes α, encouraging a bainitic transformation product, while Ni stabilizes β and promotes martensite;

3. Precipitation hardening in NAB is more significant at lower Aluminum contents and occurs at 400 to 500°C;

4. The first stages of tempering of nickel aluminum bronzes occurs at 400 to 450 °C and involves redistribution of stacking faults and annealing of dislocations (this seems to be at odds with the results of Liu and co-workers [16,17], who suggest precipitation starts at a lower temperature) and;

5. Observed structure following quenching is a function of pre-quench soak time.

Gianetto and coworkers [58] used a Gleeble to simulate microstructure development in the heat affected, reheated and as deposited regions of a laser weld. In some of their

simulations, structures similar to those in a clad surface produced by cladding a Cu-8.6 Al, 4.8 Ni, 4.0 Fe, 1.1 Mn alloy with a heat input of 1200 J/cm and a welding wire of composition Cu-9.0 Al, 4.6 Ni, 3.9 Fe and 1.2 Mn. In addition to providing a library of microstructures of known thermal history, they showed that:

1. Observed structure following quenching is a function of pre-quench soak time and starting structure;

2. Structure depended strongly upon composition. An alloy with composition Cu-8.0 Al, 4.8 Ni, 3.4 Fe and 0.66 Mn proved not to produce much martensite on quenching from the solid state, even from temperatures as high as 1030 °C;

3. GTA welds made on several nickel aluminum bronzes, with heat inputs estimated to be between 0.3 to 0.5 kJ/mm had largely Widmanstätten α deposit microstructures;

4. On rapid cooling, the transformation $\alpha + \beta \rightarrow \alpha + \beta + \kappa$ was suppressed to 855 to 875 °C depending on cooling rate and the transformation $\alpha + \beta + \kappa \rightarrow \alpha + \kappa$ was suppressed to 650 to 760 °C again, depending on cooling rate; and

5. Reheated weld metal microstructures are strongly influenced by peak temperature and cooling rate; and

6. On cooling of a simulated weld of composition Cu-9.2 Al, 4.7 Ni, 3.4 Fe, and 0.77 Mn, the formation of Widmanstätten α was suppressed by a cooling rate faster than Δt 800-500 °C equal to 1.6 seconds.

Livley and Hyatt [59] studied the tempering behavior of melt spun ribbons of nickel aluminum bronze. Optical microscopy did not reveal significant tempering at temperatures below 400 °C. An as solidified Cu-9 Al, 5 Ni, 5 Fe ribbon had a dual phase β' plus α structure while the as solidified structures of an Cu-11 Al, 5 Ni, 5 Fe ribbon and of a Cu-13 Al, 5 Ni, 5 Fe ribbon appeared to be a single phase, probably martensite, on examination with an optical microscope.

9.0 SUMMARY

A good deal of general data related to the development of microstructures during low heat input welding of nickel aluminum bronze is available and has been summarized. Data from Sections 3 and 7 show that the 9-R martensite structure predominates in the aluminum and nickel rich regions around prior κ_{II} and κ_{IV} particles, the martensites formed in the as solidified material of a low heat input weld of nominal composition Cu-10 Al, 5 Ni, 5 Fe and in as solidified material of a low heat input weld of composition Cu-9.79 Al, 2.19 Fe, 5.27 Ni. Martensites in the "retained β" regions of castings have a different structure and the binary aluminum bronzes exhibit a number of martensite variants depending on composition. Thus other structures are likely to be observed in low heat input welds of nickel aluminum bronzes of other compositions.

Data on thermodynamics and kinetics of phase transformations in these alloys is inadequate. Evidence to support the occurrence of an ordering transformation prior to the martensite transformation is conflicting. Data on a wider rage of compositions which combines microstructural work with thermal analysis on a wide range of compositions is required to answer this question. Available microstuctural data on alloys as rich as Cu-10 Al, 5 Fe, 5 Ni suggests that such an ordering transformation does not occur in these alloys, despite the thermal analysis results of Brezina [31]. It is possible that a precipitation reaction was mistaken for an ordering reaction in the thermal analysis studies which gave the CTT curves. Simulation experiments by two separate groups of workers showed that as quenched structure depends upon both soak time and temperature. Simulation experiments also showed that for a particular composition, the formation of Widmanstätten α was suppressed by a cooling rate faster than Δt 800-500°C equal to 1.6 seconds. Phase diagram data is limited especially near or above the solidus and liquidus temperatures. So is data on the effects of composition on hardenability and tempering behavior. It seems clear though that significant tempering does not occur until above temperatures of 400 °C, except at very long times. This review shows there is a lack of data and general understanding and agreement about how the Widmanstätten α phase in these alloys forms. As well it shows that there is a lack of data on the effect of heat input and composition on weld deposit structure.

10.0 REFERENCES

1. C.V. Hyatt, K.H. Magee, J. Hewitt and T. Betancourt, Laser Weld Cladding of Nickel Aluminum Bronzes, in *Abstracts and Summaries of the 2nd CF/CRAD Meeting on Naval Applications of Materials Technology*, J.R. Matthews, ed., Halifax, N.S., May 2-4, 1995

2. C.V. Hyatt, and K.H. Magee, Laser Surface Melting and Cladding of Nickel Aluminum Bronzes, in *Proceedings of Advanced Methods of Joining New Materials II*, The American Welding Society, Miami, Florida, 1994, 111-126

3. C.V. Hyatt and D.O. Morehouse. *Laser Cladding of Nickel Aluminum Bronzes: Dissimilar Metals and Complex Shapes*, DREA Technical Memorandum, in preparation, Defence Research Establishment Atlantic, Dartmouth, Nova Scotia, 1996.

4. J.A. Hewitt, *Laser Weld Overlaying of Marine Components and Alloys*, DREA CR/95/525, Defence Research Establishment Atlantic, Dartmouth, Nova Scotia, 1995.

5. D.E. Bell, Master of Science Thesis, *Microstructural Development and Corrosion Resistance of Laser-Welded Nickel Aluminum Bronze*, Pennsylvania State University, 1993.

6. K. Petrolonis, *Laser Welding and Continuous Cooling Studies of Nickel Aluminum Bronze*, Master of Science Thesis, The Pennsylvania State University, 1993

7. C.W. Draper, The Effects of Laser Surface Melting on Copper Alloys, in *Lasers in Metallurgy*, Warrendale, PA: The Metallurgical Society, 1981, 21-31

8. C.W. Draper, The Use of Laser Surface Melting to Homogenize Fe-Al bronzes, *Journal of Materials Science*, **16**, 1981, 2774 to 2780.

9. C.W. Draper, J.M. Vandenberg, C.M. Preece, and C.R. Clayton, Characterization and Properties of Laser Quenched Aluminum Bronzes. in *Rapidly Solidified Amorphous and Crystalline Alloys*. New York: Elsevier. 1982, 529-533.

10. R.J. Taylor, D.A. Weston, G.M. Wright, and B.W. Turnbull, Production of Corrosion Resistant Surfaces by Laser Processing. *Corrosion Australasia*, 1987, 12-17.

11. P.J. Oakley and N. Bailey, Laser Surfacing of Nickel Aluminum Bronze. *Proc. International Conference on Power Beam Technology* Cambridge, England, The Welding Institute, 1986, 301-314.

12. C. W. Draper and S. P. Sharma, *Thin Solid Films*, 1981, **84**, 333-340.

13. C. W. Draper, S. P.Sharma, J. L. Yeh, and S. L. Bernasek, *Surface and Interface Analysis*, 1980, **2**, 179-182.

14. C. V. Hyatt, K. Mackay, and T. Betancourt, *Materials Science and Technology, Materials Science and Technology*, 250-254, **10**, March 1994.

15. N. Dubnyakov, I. B. Malysheva, and S. F. Pulim, *Sov. J. Friction and Wear*, 1986, **7**, 70-76, Translation, New York, Allerton Press.

16. Y. Liu, J. Mazumder, and K. Shibata, Transmission Electron Microscopy Study of Martensites in Laser-Clad-Al Bronze on Aluminum Alloy AA333, *Met. Trans.* **25A**, 1994, 37-46.

17. Y. Liu, M.E. Mochel, J. Mazumder and K. Shibita, TEM Study of Precipitates in Laser Clad Ni-Al Bronze, *Acta Metall. Mater.* **42**, 1994, 1763-1768.

18. *Aluminum Bronze Alloys for Industry*, Copper Development Association, Publication No. 83, Herts, England, 1986.

19. F.L. LaQue, *Marine Corrosion*, New York, Wiley, 1975.

20. *Castings in Nickel-Aluminum Bronze, British Standard 1400-AB2-C*, London: The Mond Nickel Company Limited, 1948.

21 P.J. Macken and A.A. Smith, *The Aluminum Bronzes, Properties and Production Processes,* CDA Publication No 31, Herts, England, 1966.

22. *Rules for Building and Classing Steel Vessels.*. Paramus, New Jersey: American Bureau of Shipping Section, 1990, 37/2.

23. R.J. Ferrara and T.E. Caton, 1981. Review of Dealloying of Cast Aluminum Bronze and Nickel Aluminum Bronze Alloys in Seawater Service. *Proc. of Corrosion 81,* Paper 198. Houston, Texas: NACE.

24. E.A. Culpan, and G. Rose, Corrosion of Cast Nickel Aluminum Bronze in Sea Water, *British Corrosion Journal,* **14** 1979, 160-166.

25. Rowlands, J.C. and Brown, T.R.H.M. Preferential Phase Corrosion of Cast Aluminum Bronzes with Complex Microstructure in Seawater. *Proc. 4th International Congress on Marine Corrosion and Fouling,* Juan les Pins, France, 1976, 475-479.

26. J.C. Rowlands, Studies on the Preferential Phase Corrosion of Cast Nickel Aluminum Bronze in Seawater, *Proc. 8th International Congress on Metallic Corrosion,* 1981, 1346-1351. Mainz, Germany.

27. P.J. Barnes, An Assessment of the in-Service Corrosion Performance of Nickel Aluminum Bronze Castings, in *Proceedings of the 8th Inter-Naval Corrosion Conference*, RNEC, Manadon, England, 1988.

28. *Guidance Notes for Welding Aluminum Bronze*, CDA Publication No 80, Herts, England, 1980.

29. Naval Engineering Standard 747, *Requirements for Nickel Aluminum Bronze Castings and Ingots*, Part 2, Issue 2, Ministry of Defence, Bath, England, 1987.

30. M. Sahoo and A. Coutre, *Microstructure and Mechanical Properties of Continuously cast Mn-Ni-Al Bronzes*, Physical Metallurgy Laboratories Report, MRP/PMRL, 83-6(OP-J), CANMET, 588 Booth Street, Ottawa, Canada, 1983.

31. P. Brezina, Heat Treatment of Complex Aluminum Bronzes, International Metals Reviews, 1982, **27**, 77-121.

32. E. A. Culpan and G. Rose, Microstuctural Characterization of Cast Nickel Aluminum Bronze, *Journal of Materials Science* **13**, 1978, 1647-1657.

33. F. Hasan, A. Jahanafrooz, G.W. Lorimar, and N. Ridley, 1982. The Morphology, Crystallography, and Chemistry of Phases in As-Cast Nickel-Aluminum Bronze. *Metallurgical Transactions* **13A** 1337-1345.

34. A.K. Sinha, *Ferrous Physical Metallurgy*, Boston, Butterworths, 1989.

35. P. Weill-Couly and D. Armaund, Influence de la Composition et de la Structure des Cupro-Aluminums sur leur Comporment en Service, *Fonderie* **322**, 1973, 123-135.

36. R. Thompson and J. O. Edwards, The Kappa Phase in Nickel Aluminum Bronze, Part 1: Slow cooled Microstructures, *82nd Annual meeting of the American Foundarymans's Society*, 1978, 385-394.

37. F. Hasan, G.W. Lorimar and N. Ridley, Tempering of Cast Nickel-Aluminum Bronze, *Metals Science*, **17**, 1983, 289-295.

38. M. Cook, W.P. Fentiman and E. Davis, 1952, Observations on the Structure and Properties of Wrought Copper-Aluminum-Nickel-Copper Alloys, *Journal of the Institute of Metals*, **80**, 419-429.

39. F. Hansan, G.W. Lorimar and N. Ridley, Phase Transformations During Welding of Nickel Aluminum Bronze, in *Proceedings Conference on Phase Transformations*, Cambridge, U.K., 1987, 131-134.

40. C.M. Wayman, *Introduction to the Crystallography of Martensitic Transformations*, Macmillan, New York, 1964.

41. *Alloy Phase Diagrams, ASM Handbook*, Volume 3, ASM, Materials Park, Ohio, 1992.

42. P. Brezina, Gefügeumwandlungen und mechanische Eigenscaften der Mehrstoff-Aluminumbronzen vom Typ CuAl 10 Fe5 Ni5,*Giessseri-Forshung*, 1973, 1-10.

43. M. Kanamori, S. Ueda, and S. Matsuo, On the Structures of Cu-Al-Ni-Fe alloys. (Nickel Aluminum Bronze for Marine Propeller Alloys, 1st Report) **4**, 1959, 201-213.

44. V.H. Rhininsland and E. Wachtel, Über den Aufbau und die Magnetichen Eigenschaten von Festen und Flüssigen Kupfer-Aluminum-Legierungen mit Zusätzen von Übergangs Metallan, *Giesserei Forscung*, **22**, 1970, 1-14.

45. G.F. Vander Voort, Editor, *Atlas of Time-Temperature Diagrams for Nonferrous Alloys*, ASM, Materials Park, Ohio, 1991.

46. J.R. Moon and R.D. Garwood, Transformations During Continuous Cooling of the β Phase in Copper-Aluminum Alloys, *Journal of the Institute of Metals*, 1986, 17-21.

47. L. S. Euken, P. Donner and E. Hornbogen, Temperature and Stress induced austenite-martensite and martensite-martensite transformation in rapidly quenched shape memory alloys, *Proceedings of Phase Transformations '87*, The Institute of Metals, London, England, 1988, 174-177.

48. H. Goldstein and I.G.S Fallerios, Isothermal Decomposition of the β_1' Martensite in Cu-Al: Morphological Study. *ICOMAT 1979: Martensitic Transformations*, MIT, Cambridge, Mass. 1979, 566-571.

49. D.J. Mack, Isothermal Transformation of Eutectoid Aluminum Bronze, *Trans. AIME*, **175**, 1948, 241-261.

50. D.E. Bell, K. Petrolonis and P.R. Howell, Solid-Solid Phase Transformations in Laser Welded Aluminum Bronzes, in *International Trends in Welding Science and Technology*, S.A. David and J.M. Vitek, Gatlinburg, TN, 1992, 301-305.

51. D. E. Bell, T.A. Marsico, K. Petrolonis, P. E. Denney and P.R. Howell, The Microstructures of Laser Welded Aluminum Bronzes, in Metallography: past, Present and Future, ASTM STP 1165, G.F. Vander Voort, F.J. Warmoth, S.M. Purdy and A. Szirmae, Eds. ASTM, Philadelpia , Penn., 1995, 327-434.

52. M. Sahoo, *Weldability of Nickel Aluminum Bronze Alloy UNS C95800*, Physical Metallurgical Research Laboratories Report MRP/PMRL 81-83 (Op-J), CANMET, 588 Booth Street, Ottawa, Canada, 1983.

53. M. Sahoo, Weldability of Nickel Aluminum Bronze Alloy C95800, AFS Transactions, **112**, 1982, 893-911.

54. G. Newcombe, C. Dimbylow, R. Jones, in *Welding of Castings*, The Welding Institute, Bradford, England, 1976, 199-216.

55. *Memorandum for the weld repair of nickel aluminum bronze and copper nickel castings.* S&S Engineering Consultants Report, Kent, England, 1988.

56. *Requirements and procedure and inspection for weld repair of copper alloy and nickel alloy castings*, Naval Engineering Standard NES 771, Issue 1, July 1991.

57. C. Bennet and C.V. Hyatt, *Characterization of Laser Clad Nickel Aluminum Bronze with Analytical Electron Microscopy*, To be Published.

58. J.A.Gianetto, M.Sahoo, M.W. Letts and C.Bibby, *The Microstructural Characterization of NiAl Bronze Weldments DREA,* CR/95/435, Defence Research Establishment Atlantic, Dartmouth, Nova Scotia

59. K.A. Livley and C.V. Hyatt, Characterization of Melt Spun Ribbons of Nickel Aluminum Bronze, Informal report, Defence Research Establishment Atlantic, Dartmouth, Nova Scotia.

UNCLASSIFIED

SECURITY CLASSIFICATION OF FORM
(highest classification of Title, Abstract, Keywords)

DOCUMENT CONTROL DATA

(Security classification of title, body of abstract and indexing annotation must be entered when the overall document is classified)

1. ORIGINATOR (The name and address of the organization preparing the document. Organizations for whom the document was prepared, e.g. Establishment sponsoring a contractor's report, or tasking agency, are entered in section 8.)

Defence Research Establishment Atlantic
P.O. Box 1012, Dartmouth, N.S. B2Y 3Z7

2. SECURITY CLASSIFICATION (Overall security of the document including special warning terms if applicable.)

UNCLASSIFIED

3. TITLE (The complete document title as indicated on the title page. Its classification should be indicated by the appropriate abbreviation (S,C,R or U) in parentheses after the title.)

Review of Literature Related to Microstructural Development During Laser Surface Engineering of Nickel Aluminum Bronze

4. AUTHORS (Last name, first name, middle initial. If military, show rank, e.g. Doe, Maj. John E.)

Hyatt, Calvin V.

5. DATE OF PUBLICATION (Month and year of publication of document.)

March 1997

6a. NO. OF PAGES (Total containing information. Include Annexes, Appendices, etc.)

31

6b. NO. OF REFS. (Total cited in document.)

59

6. DESCRIPTIVE NOTES (The category of the document, e.g. technical report, technical note or memorandum. If appropriate, enter the type of report, e.g. interim, progress, summary, annual or final. Give the inclusive dates when a specific reporting period is covered.)

Technical Memorandum

8. SPONSORING ACTIVITY (The name of the department project office or laboratory sponsoring the reseach and development. include the address.)

Defence Research Establishment Atlantic
P.O. Box 1012, Dartmouth, N.S. B2Y 3Z7

9a. PROJECT OR GRANT NUMBER (If appropriate, the applicable research and development project or grant number under which the document was written. Please specify whether project or grant.)

1.f.a

9b. CONTRACT NUMBER (If appropriate, the applicable number under which the document was written.)

10a. ORIGINATOR'S DOCUMENT NUMBER (The official document number by which the document is identified by the originating activity. This number mrst be unique to this document.)

DREA Technical Memorandum 96/227

10b. OTHER DOCUMENT NUMBERS (Any other numbers which may be assigned this document either by the originator or by the sponsor.)

11. DOCUMENT AVAILABILITY (Any limitations on further dissemination of the document, other than those imposed by security classification)

(X) Unlimited distribution
( ) Distribution limited to defence departments and defence contractors; further distribution only as approved
( ) Distribution limited to defence departments and Canadian defence contractors; further distribution only as approved
( ) Distribution limited to government departments and agencies; futher distribution only as approved
( ) Distribution limited to defence departments; further distribution only as approved
( ) Other (please specify):

12. DOCUMENT ANNOUNCEMENT (Any limitation to the bibliographic annoucement of this document. This will normally correspond to the Document Availability (11). However, where futher distribution (beyond the audience specified in 11) is possible, a wider announcement audience may be selected.)

UNCLASSIFIED

SECURITY CLASSIFICATION OF FORM

DCDO3 2/06/87

13. ABSTRACT (a brief and factual summary of the document. It may also appear elsewhere in the body of the document itself. It is highly desirable that the abstract of classified documents be unclassified. Each paragraph of the abstract shall begin with an indication of the security classification of the information in the paragraph (unless the document itself is unclassified) represented as (S), (C), (R), or (U). It is not necessary to include here abstracts in both official languages unless the text is bilingual).

In this report, literature related to the low heat input welding of nickel aluminum bronze is examined. This includes data on phases present, composition effects, phase diagrams, transformation kinetics, and the nature of martensites. Relevant data on microstructure development in castings, wrought materials, conventional welds and low heat input welds is considered. So is related work on the examination of melt spun ribbons and Gleeble studies. Available data show that a martensite with a 9-R structure is common in low heat input nickel aluminum bronze welds over a range of compositions. Other structures are expected at other compositions. Data also show that for at least one alloy composition, formation of Widmanstätten α can be suppressed with a high enough cooling rate ($\Delta t_{800\text{-}500}$ of 1.6 seconds or faster). As well, data show that tempering of martensites in weld heat affected zones probably does not occur at temperatures of less than roughly 400 °C. The review shows that experiments to obtain data on ordering, metastable reactions, precipitation and tempering are needed. Also needed are experiments to understand the effect of composition and heat input on microstructure.

14. KEYWORDS, DESCRIPTORS or IDENTIFIERS (technically meaningful terms or short phrases that characterize a document and could be helpful in cataloguing the document. They should be selected so that no security classification is required. Identifiers, such as equipment model designation, trade name, military project code name, geographic location may also be included. If possible keywords should be selected from a published thesaurus. e.g. Thesaurus of Engineering and Scientific Terms (TEST) and that thesaurus-identified. If it not possible to select indexing terms which are Unclassified, the classification of each should be indicated as with the title).

Laser Cladding
Welding
Nickel Aluminum Bronze
Phase Transformation
Surface Melting
Low Heat Input Welding